Human Molecular Genetics, 2008, Vol. 17, No. 2 **256–265**
doi:10.1093/hmg/ddm302
Advance Access published on October 18, 2007

Alpha-cardiac actin mutations produce atrial septal defects

Hans Matsson[1], Jacqueline Eason[2], Carol S. Bookwalter[3], Joakim Klar[1], Peter Gustavsson[1], Jan Sunnegårdh[4], Henrik Enell[5], Anders Jonzon[6], Miikka Vikkula[7], Ilse Gutierrez[7], Javier Granados-Riveron[2], Mark Pope[2], Frances Bu'Lock[8], Jane Cox[8], Thelma E. Robinson[2], Feifei Song[2], David J. Brook[2], Steven Marston[9], Kathleen M. Trybus[3] and Niklas Dahl[1,*]

[1]Department of Genetics and Pathology, The Rudbeck Laboratory, Uppsala University and University Hospital, S-75185 Uppsala, Sweden, [2]Institute of Genetics, University of Nottingham, Queen's Medical Centre, NG7 2UH Nottingham, UK, [3]Department of Molecular Physiology and Biophysics, University of Vermont, VT 05405 Burlington, USA, [4]The Queen Silvia Children's Hospital, S-416 85 Göteborg, Sweden, [5]Department of Pedriatics, County Hospital of Halmstad, S-301 85 Halmstad, Sweden, [6]Children's Hospital, Uppsala University, S-75185 Uppsala, Sweden, [7]Human Molecular Genetics (GEHU), Christian de Duve Institute, Université catholique de Louvain, B-1200 Brussels, Belgium, [8]Department of Pediatric Cardiology, Glenfield Hospital, LE3 9QP Leicester, UK and [9]National Heart and Lung Institute, Imperial College, SW3 6LY London, UK

Received August 28, 2007; Revised and Accepted October 10, 2007

Atrial septal defect (ASD) is one of the most frequent congenital heart defects (CHDs) with a variable phenotypic effect depending on the size of the septal shunt. We identified two pedigrees comprising 20 members segregating isolated autosomal dominant secundum ASD. By genetic mapping, we identified the gene-encoding alpha-cardiac actin (ACTC1), which is essential for cardiac contraction, as the likely candidate. A mutation screen of the coding regions of *ACTC1* revealed a founder mutation predicting an M123V substitution in affected individuals of both pedigrees. Functional analysis of ACTC1 with an M123V substitution shows a reduced affinity for myosin, but with retained actomyosin motor properties. We also screened 408 sporadic patients with CHDs and identified a case with ASD and a 17-bp deletion in *ACTC1* predicting a non-functional protein. Morpholino (MO) knockdown of ACTC1 in chick embryos produces delayed looping and reduced atrial septa, supporting a developmental role for this protein. The combined results indicate, for the first time, that ACTC1 mutations or reduced ACTC1 levels may lead to ASD without signs of cardiomyopathy.

INTRODUCTION

Failure of atrial or ventricular septation accounts for nearly 50% of congenital cardiovascular diseases diagnosed in 1% of newborns. Secundum ASD [MIM 108800] is characterized by an incomplete closure of the ostium secundum resulting in a left-to-right shunting of oxygenated blood. The septal defects in affected cases display a variable range of phenotypic effects depending on the size of the shunt and may result in pulmonary hypertension, right heart volume overload and premature heart failure (1,2). In most cases, the septal shunt can be closed by open-heart surgery and/or catheter intervention. It requires no further treatment.

Recently, heterozygous mutations in several transcription factors expressed in heart, such as NKX2-5, TBX5 and GATA4, have been reported in patients with ASD (3–5). A reduced or abolished function in one of the transcription factors of importance for cardiogenesis will also affect the downstream target genes. One family with isolated ASD has been identified with a mutation in alpha-myosin heavy chain (*MYH6*), a cardiac specific gene under the control of TBX5 (6).

*To whom correspondence should be addressed at: Department of Genetics and Pathology, The Rudbeck Laboratory, Uppsala University, 751 85 Uppsala, Sweden. Tel: +46 18 611 2799; Fax: +46 18 554025; Email: niklas.dahl@genpat.uu.se

Here, we report on the genetic linkage analysis in two large families segregating autosomal-dominant isolated ASD. Altogether 20 family members were diagnosed with ASD, of which several individuals have an asymptomatic septal shunt. The results from genetic linkage revealed a genomic region on chromosome 15q13–q21 spanning the gene encoding alpha-cardiac actin (*ACTC1*), which is the predominant actin in embryonic heart. Screening for *ACTC1* mutations in the two families as well as in a separate sporadic patient cohort with congenital heart defect (CHD) revealed two distinct allele variants. These variants were subsequently analyzed using a purified ACTC1 *in vitro* system with a missense mutation associated with ASD and a knockdown of ACTC1 in chick embryos, which mimics the predicted effect from an *ACTC1* deletion found in one patient with ASD. The combined results show that ACTC1 is critical for normal cardiac morphogenesis and that both structural alterations and reduced levels of ACTC1 may lead to failure of the atrial septum to close.

RESULTS

A single ACTC1 missense mutation linked to atrial septum defect in two pedigrees

We identified two large families of Swedish origin segregating isolated secundum ASD with variable clinical expression. Diagnosis was confirmed by echocardiography and the penetrance appeared complete (Fig. 1). Cardiomyopathy or other cardiovascular anomalies were excluded in all affected individuals, and several family members with ASD have a subclinical phenotype as result of a small shunt that was diagnosed by echocardiography.

To identify the gene defect underlying ASD, we genotyped members of Family 1 using microsatellite markers on all autosomes. A specific haplotype was identified in all affected individuals spanning a 15.1-cM (12.2 Mb) region of chromosome 15q13–q21 flanked by markers *D15S1040* and *D15S659* (Fig. 1). We extended the analysis to Family 2 using two novel polymorphic repeats: *GT44248* and *GATA12322*. A minimal haplotype with significant linkage to ASD (Table 1) was identified, consisting of markers *GT44248–GATA12322–ACTC*. All affected individuals available for genotyping have identical allele sizes for the marker haplotype, suggesting a shared ancestral mutation for the two families. A two-point logarithm of odds (LOD) score of 4.8 (Θ=0) was obtained for marker *ACTC* (Table 1) located within intron 4 of the gene encoding *ACTC1*. The haplotype spans a region that contains ~20 other genes, some of which may be cardiac expressed but none of which represent a strong candidate gene compared with *ACTC1*. Sequence analysis of *ACTC1* revealed a heterozygous A to G transition at cDNA position 373 from the initiator Met (Fig. 2A) in all of the 20 available affected individuals as well as in individual 14 from Family 1 who shares the linked marker haplotype with the affected individuals. The mutation is located in exon 2 and predicts an M123V substitution in the mature cardiac actin. The methionine and cystein residues are removed during actin processing and the amino acids in ACTC1 are numbered starting at the aspartic acid residue (7).

A 17-bp ACTC1 deletion associated with ASD

To screen for *ACTC1* mutations in the cases of mainly sporadic CHD, we analyzed the coding regions of *ACTC1* in a cohort of 408 individuals referred to regional pediatric cardiology clinics in Sweden, Belgium and the UK. A 10-year-old female with a secundum ASD was found to be heterozygous for a 17-bp deletion in exon 2 (corresponding to nucleotides 215–231 in cDNA; Fig. 2B). Studies in the extended family revealed the deletion on one *ACTC1* allele also in the patient's 43-year-old father, who had no previous history of CHD. Further clinical assessment showed that the father had an abnormal echocardiogram with a posteriorly deviated interventricular septum, thought to be associated with a spontaneously closed perimembranous ventricular septal defect, causing aortic valve regurgitation. The electrocardiogram was normal. This deletion in *ACTC1* is predicted to lead to a severely truncated protein 86 amino acids in length compared with the mature wild-type (WT) ACTC1, which has 375 amino acids (7). Neither this deletion nor the A to G transition at cDNA position 373 was found in the rest of the cohort or in 580 control samples.

Biochemical studies show reduced affinity of M123V actin for myosin *in vitro*

To study the functional consequences of the M123V cardiac actin substitution, we performed an analysis on recombinant WT and mutant ACTC1 obtained from a baculovirus/Sf9 cell system (8). The steady-state actin-activated ATPase activity of β-cardiac myosin was determined as a function of increasing actin concentrations for WT and M123V actins at 50 mM NaCl (Fig. 3A). K_m for myosin was ~2-fold higher for M123V actin compared with the WT actin, indicating that the mutant actin has a lower affinity for myosin than does the WT actin. V_{max} of the two actins differed by ~20% (WT, $0.81 \pm 0.04\ s^{-1}$; M123V, $1.03 \pm 0.1\ s^{-1}$). Then, we then analyzed the relative binding of M123V actin to alpha-actinin. A competitive binding assay showed that the M123V actin does not have a decreased affinity for alpha-actinin compared with normal actin. Figure 3B shows an average of two independent experiments. We also assessed the effect of the mutation on actomyosin's motor properties by the *in vitro* motility assay (Fig. 3C). The velocity at which the mutant M123V actin was moved by cardiac myosin (1.22 ± 0.02 μm/s) was not significantly different to that seen with WT actin (1.24 ± 0.02 μm/s). These experiments suggest a relative mild and specific effect of the M123V actin with reduced affinity for myosin compared with WT actin. However, the M123V actin retains a normal actin filament polymerization ability and normal actomyosin motor function *in vitro*.

MO knockdown of ACTC1 in chick embryos leads to delayed bulboventricular looping and reduced atrial septa

The functional consequences of the 17-bp *ACTC1* deletion were analyzed, and we hypothesized that the deletion results in haploinsufficiency for ACTC1. The severely truncated ACTC1 would be non-functional or absent because of

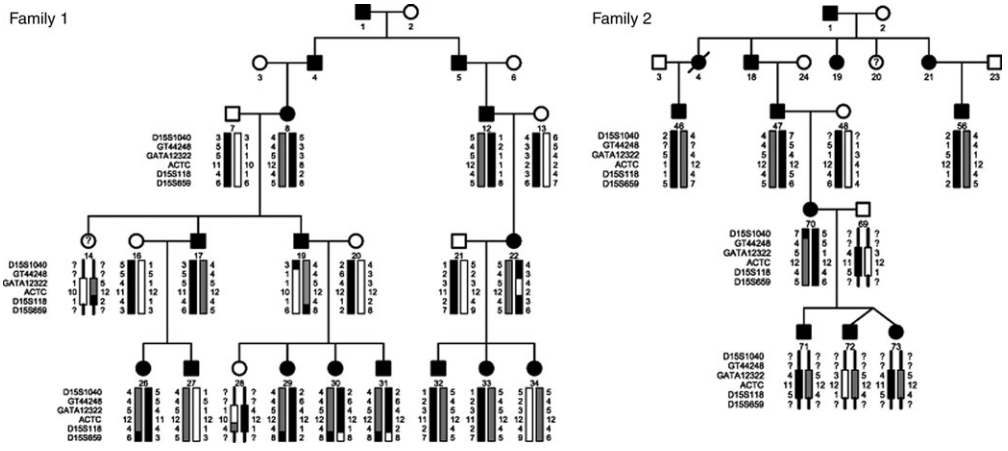

Figure 1. Genetic analysis of two Swedish pedigrees segregating isolated autosomal dominant ASD. Pedigrees with marker haplotypes on chromosome 15q13–q21 linked to ASD are indicated as grey bars with marker loci to the left of each generation. Filled symbols denote individuals affected by ASD, white symbols are unaffected family members and symbols with a question mark denote phenotype unknown.

Table 1. Cumulative two-point logarithm of odds score at different recombination fractions (Θ) for each marker locus on chromosome 15 segregating with ASD in all affected members of Families 1 and 2

Marker	Recombination frequency (cM)[a]	Physical position (Mb)	LOD score at Θ				
			0.0	0.1	0.2	0.3	0.4
D15S1040	28.35	31.91	−4.8	1.6	1.5	1.1	0.6
GT44248[b]	–	32,80	3.9	3.1	2.3	1.5	0.8
GATA12322[b]	–	32,81	4.9	3.9	2.9	2.0	1.0
ACTC	31.46	32.87	4.8	3.9	2.9	1.9	0.9
D15S118	32.58	34.02	−∞	1.5	1.4	1.0	0.5
D15S659	43.47	44.16	−∞	0.6	0.8	0.6	0.4

The genetic recombination frequency in centiMorgan and the physical position in Megabases for each marker are given in columns 2 and 3, respectively.
[a]Genetic distance according to Marshfield sex-averaged genetic map.
[b]Novel characterized polymorphic dinucleotide repeats.

nonsense mediated decay of the mutant transcript resulting in an impaired development of the heart. To test this hypothesis, we performed MO knockdown in chick embryos at Hamburger Hamilton (HH) stage 13–14 (9). Following MO knockdown, ACTC1–MO embryos had shorter, less-developed atrial septa than WT embryos (Fig. 4). Of the control hearts, 12 of 14 had well-developed septa, compared with the ACTC–MO treated embryos in which none of the seven had a well-developed septum. This difference is significant (Fischer's exact test, $P < 0.001$). Our results also show that a reduction in cardiac alpha-actin delays s-looping of the early chick heart. We found that 3 out of 14 control embryos appeared to have delayed looping compared with five out of seven ACTC–MO-treated embryos. This difference is also statistically significant (Fischer's exact test, $P < 0.05$). This is consistent with previous reports that have shown that actin polymerization plays an important part in early looping of the avian heart, the so-called c-looping that occurs by HH Stage 12 (10,11).

DISCUSSION

In this study, we have identified dominant *ACTC1* gene mutations in patients with isolated ASD. The mutations are associated with a marked clinical variability from an asymptomatic shunt to a severe cardiac decompensation treated by surgery. None of the affected individuals were diagnosed with cardiomyopathy. Patients with contiguous gene syndromes and chromosome 15q deletions spanning the *ACTC1* gene have been reported previously (12). Several of these patients present with CHD including ASD, suggesting a gene locus of importance for cardiac septal formation on chromosome 15q. Furthermore, a recent study by Monserrat *et al.*(13) identified septal defects in some individuals with cardiomyopathy and ACTC1 mutations.

*ACTC1*s are the major component of the sarcomeric thin filaments and are essential for cardiac muscle contraction. Each myosin head interacts with two adjacent actin monomers along the cardiac filament structure (F-actin). The binding sites are within subdomain 1, which is located on the outer lobe of the actin monomer. Subdomain 1 also interacts with other sarcomeric proteins including troponin, tropomyosin and alpha-actinin (14). The Met-123 is completely buried in the hydrophobic core of subdomain 1 and is therefore not in a position to interact with other proteins (Fig. 5A and B). Although the M123V involves a conservative substitution of a hydrophobic amino acid, the change from a straight to a branched aliphatic side chain may alter the tight packing of the hydrophobic core of subdomain 1 leading to a change in

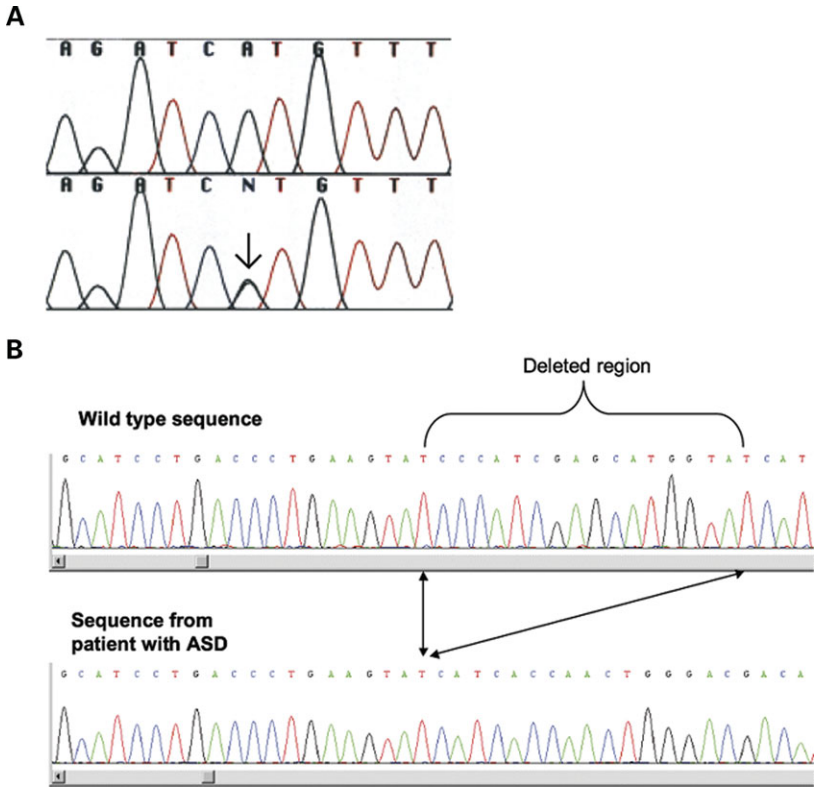

Figure 2. Two different cardiac alpha actin mutations found in individuals affected by isolated ASD. (**A**) Sequence chromatogram from a normal individual (upper part) and from an affected individual illustrating the *ACTC1* exon 2 mutation at cDNA position 373 (373A to G, lower part depicted by arrow) predicting an M123V substitution. Signals from both alleles showing an A and a G, respectively, are shown. (**B**) Sequence trace of cloned amplicons spanning exon 2 of *ACTC1* from a normal individual (top) compared with the *ACTC1* exon 2 from a patient with a secundum ASD and a 17-bp deletion (bottom). Signals from a single allele are shown.

the shape of the subunit or in its flexibility. This may explain why M123V actin presents a reduced affinity for myosin in the presence of ATP. The ability of the mutant actin to be moved by cardiac myosin at the same rate as WT actin suggests that the mutation does not affect the rate of ADP release from myosin. This assay also rules out the possibility that the M123V mutation prevents the assembly of actin monomers into a filamentous polymer that can support the movement by myosin. The results suggest a relative mild and specific effect of the M123V actin compared with WT actin.

Amino acid substitutions in ACTC1 were previously described in individuals with primary hypertrophic cardiomyopathy (HCM [MIM 192600]) or dilated cardiomyopathy (DCM [MIM 115200]) (15–19). These mutations are exposed to the actin surface and located within or in close proximity to binding sites for myosin or to other actin binding proteins. The M123V mutation, however, is not associated with cardiomyopathy in our families. In contrast, the cardiac phenotype is restricted to variable degrees of ASD secundum. More severely affected family members were treated by cardiac surgery during the first years of life because of cardiac decompensation, whereas milder cases have a sub-clinical phenotype diagnosed in adulthood during this study. One ACTC1 mutation, E99K, associated with cardiomyopathy was recently shown to have a pronounced effect on the affinity of actin for myosin (8). Interestingly, the E99K cardiac actin also showed a consistently lower *in vitro* motility compared with WT cardiac actin, which is likely related to the lower average force supported by the mutant actin (8). In combination with our findings, this supports that ACTC1 mutations with intact actomyosin motor properties do not lead to cardiomyopathy.

Actins are highly conserved proteins and Met-123 is conserved in animal, plant and fungal actin. Mutations in skeletal actin (ACTA1), which is co-expressed with ACTC1 in adult heart, are associated with muscle myopathies including actin myopathy [MIM 102610] and nemaline myopathy (NM) (NEM3 [MIM 161800]), characterized by muscle fiber abnormalities and muscle weakness (20). With a few exceptions, the *ACTA1* gene mutations do not cause a cardiac phenotype (21,22). One conservative mutation of a hydrophobic amino acid in the core of subdomain 1, I357L, is associated with NM (23). Furthermore, one *ACTA1* mutation in a patient with mild NM results in an M132V substitution, which reduces actin polymerization ability *in vitro* (24). Interestingly, the crystal structure of monomeric actin shows that the Met-132 residue is located in close proximity to the Met-123 within the core of subdomain 1 (Fig. 5C). However, in our study, no actin polymerization defect was found for the recombinant M123V actin, suggesting that the position of the mutated residue within the actin subdomain 1 is important for the shape and stability of the subunit.

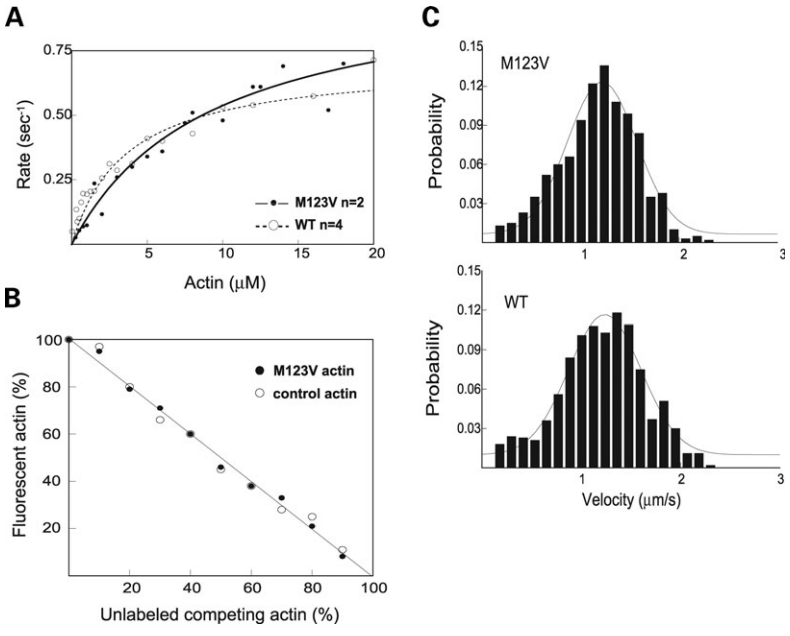

Figure 3. Functional studies of the M123V mutated alpha cardiac actin. (**A**) The steady-state actin-activated ATPase activity of myosin was measured as a function of actin concentration. Cardiac myosin was used in conjunction with expressed WT (open circles) or M123V (filled circles) actin. Data were fit to the Michaelis–Menten equation. The M123V actin showed a higher K_m for cardiac myosin (9.21 ± 2.11 μM) compared with the WT actin (4.70 ± 0.71 μM). The V_{max} of the two actins were similar (WT, 0.81 ± 0.04 s^{-1}; M123V, 1.03 ± 0.1 s^{-1}). (**B**) The relative binding of actin to alpha-actinin was determined using a competitive binding assay in a flow cell. Binding of fluorescent phalloidin-labeled actin (M123V mutant or tissue-purified actin) to alpha-actinin was competed with increasing amounts of unlabeled-phalloidin tissue-purified actin (control). The unlabeled actin displaced both M123V (fille circles) and tissue-purified actin (open circles) proportionately to the dilution made, showing that the mutant actin does not have a decreased affinity for alpha-actinin. (**C**) The analysis of an *in vitro* motility assay for measurement of M123V and WT actins sliding velocity using cardiac myosin. The velocities observed with expressed WT actin were near identical as with the mutant M123V. Gaussian fit for 202 filaments of M123V actin was 1.22 ± 0.02 and 1.24 ± 0.02 μm/s for 171 filaments of WT actin.

In the present study, we also identified a patient with isolated ASD and a 17-bp deletion in *ACTC1*, which predicts a non-functional protein. Our results from knockdown of ACTC1 in chick show less developed atrial septa supporting a dosage-dependant effect of ACTC1 on cardiac development. This is also consistent with previous studies showing that actin polymerization plays an important part in early avian heart development (25–27). Mice lacking cardiac actin do not survive >2 weeks (28). Hearts are apparently normal at the level of gross morphology, but increased apoptosis was found in the atrial and ventricular walls at fetal day 17 (29). It has been suggested that the lack of *ACTC1* may induce apoptosis leading to disrupted cardiac differentiation. Apoptosis plays a crucial role in embryological development and excessive absorption/apoptosis of the primary septum is thought to be a cause of secundum ASDs. In humans, development of the septum secundum occurs when a fold in the atrial wall grows out into the primitive atrium (30). Atrial septal defects occur either because of incomplete growth of the septum secundum or because of increased absorption of the septum primum. It is noteworthy that *ACTC1* is essentially the only actin in embryonic heart muscle (31,32). In the adult heart, 20% of actin is skeletal muscle actin and it is possible that the co-polymerization of cardiac and skeletal actins could compensate for a negative affect of a cardiac actin mutation. In mice, transgenic expression of smooth muscle γ-actin partially rescues the ACTC1 null mutant mouse (28). Furthermore, in BALB/c mice, a duplication of the promoter and three first exons result in a reduced cardiac actin expression and abnormally high accumulation of the skeletal actin transcripts (33). This co-regulation of cardiac and skeletal actins seems to be present also in humans as ACTC1 was found to be upregulated in skeletal muscle sufficient for survival in a patient with an ACTA1 null phenotype (34) A similar mechanism with upregulation of ACTA1 would, in part, explain the absence of adult cardiomyopathy in certain individuals expressing mutant ACTC1 leading to truncated non-functional proteins.

In summary, we propose that reduced levels or impaired function of ACTC1 at a crucial stage in development leads to a delayed looping of the heart and prevents normal septal development, resulting in an ASD. Actin knockdown in chick embryos produces reduced atrial septation and *in vitro* analysis of M123V actin shows that the cardiac actin mutation perturbs some aspect of contractile function. Thus, the ASDs as a result of M123V mutation or protein truncation/depletion would involve a similar mechanism to that recently reported for the MYH6 mutation (6). In each case, major structural proteins of the heart play a dual role. They are required for normal contractile function and specific substitution mutations lead to dilated cardiomyopathy and HCM. These proteins also play a key role in cardiac morphogenesis where a different spectrum of mutations results in CHDs. Finally, isolated secundum ASD is a common heart malformation affecting 1/1500 live births of which ~10% are familial (35). In such cases, *ACTC1* may serve as a candidate for

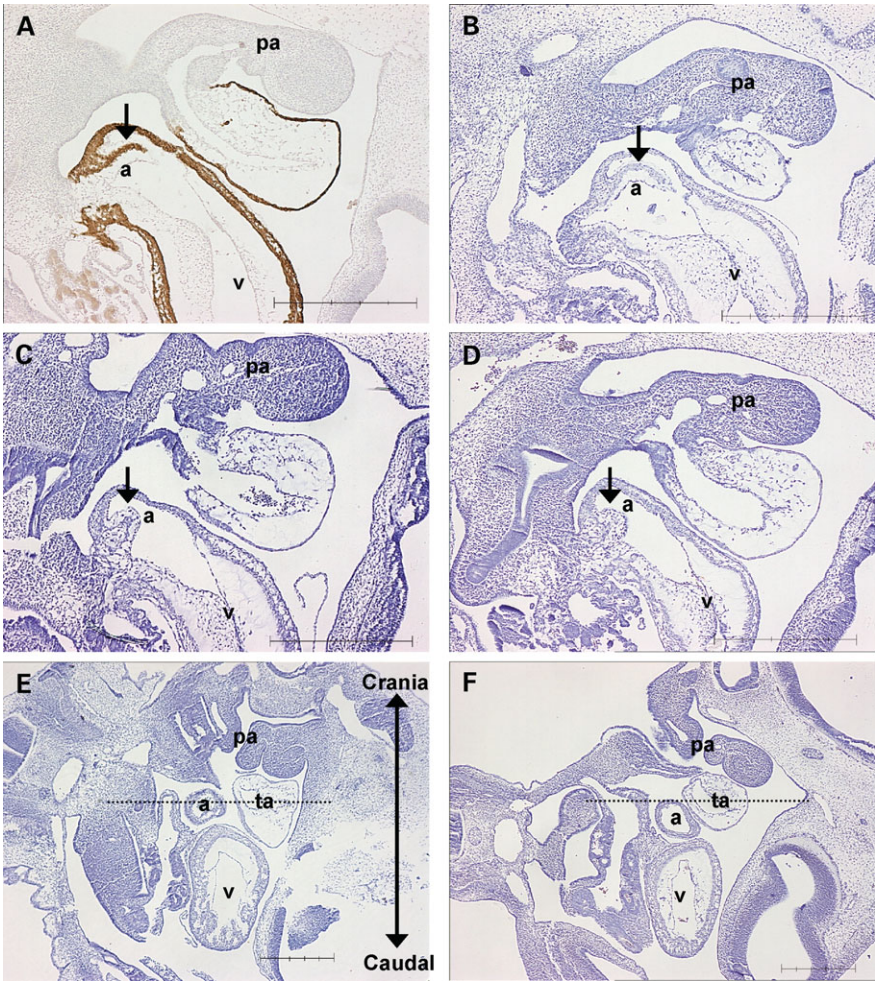

Figure 4. Knockdown of ACTC1 leads to reduced septation and delayed cardiac looping in the chick. Sagittal sections of chick hearts at HH Stage 20–21 are shown at ×5 magnification (**A–D**) The sections were stained using Mayers Haemalum (**A–F**) and treated with a monoclonal antibody against chicken alpha-cardiac actin (A). (A) and (B) Wild-type embryo hearts treated with pluronic gel only. (C) and (D) Embryos treated with ACTC1 morpholino (MO) showing reduced septal size (shown by arrows). Examples of WT (E) and ACTC1 MO-treated embryos (F) are shown at ×2.5 magnification. It can be seen from the dotted line that the relations between the atrium and the truncus arteriosus differs in (E) and (F) indicative of a looping problem. The features are not seen in the WT or other control embryos after correction for embryo age at application of MO. a, atrium; v, ventricle; ta, truncus arteriosus; pa, pharyngeal arches. (The cranial/caudal orientation labelled in (E) applies to all embryo sections.)

diagnostic or pre-symptomatic screening and for improved genetic counseling.

MATERIALS AND METHODS

Patients

All individuals included in this study were ascertained through investigations at departments of cardiology/paediatric cardiology and by patient files. Individual 1:14 in Family 1 (Fig. 1) is not available for cardiac examination and was therefore typed with a phenotype unknown with respect to ASD. Cardiac examinations of individual Family 1:28 revealed no signs of ASD, whereas the father (1:19) has a persistent ASD. Individual Family 1:29 was diagnosed with a small ASD 2 months after birth but the septum was closed at age 14 months. This patient was considered affected. Individual 1:12 (Family 1) was diagnosed with cardiac decompensation due to persistent ASD, which is surgically corrected. The daughter (1:22) has also undergone cardiac surgery for ASD. Individuals 1:32 and 1:33 were diagnosed and surgically corrected for large secundum ASD, whereas 1:34 was diagnosed with a small ASD that spontaneously closed before the examination 11 months later. In Family 2 (Fig. 1), the mother (2:70) was diagnosed with symptomatic secundum ASD subsequently corrected by surgery. Her children were diagnosed with moderate secundum ASD (2:71) and small secundum ASD (2:72 and 2:73). All three children are clinically compensated at age 3–7 years. Individuals in the first generations of Family 2 have been described previously (36). Affected family members had no other associated heart malformations, and cardiomyopathy was excluded in affected individuals with an asymptomatic ASD as well as in family members who were surgically treated for cardiac decompensation. Cases affected by isolated ASD and other non-syndromic CHD were recruited from outpatient clinics in Sweden, Belgium

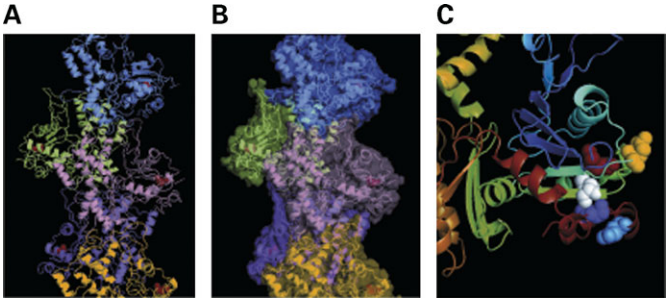

Figure 5. Front view of polymeric actin rendered using MacPymol. The Met-123 residues are indicated in red (**A–C**). (A) Ribbon representation with each actin monomer in different color. (B) Surface rendering superimposed on ribbon representation showing that Met-123 is buried within subdomain 1. (C) Ribbon representation of monomeric actin showing subdomain 1 and the relationship of ACTC1 Met-123 (red) to the ACTA1 Met-132 (white) and Ile-357 (purple) amino acids that are associated with nemaline myopathy. The ACTC1 surface residues associated with cardiomyopathy is represented by blue spheres (Glu-99) and by yellow spheres (Asp-361).

and the UK based at a tertiary referral center for pediatric cardiology. The cohort comprised 408 cases and included 86 individuals with secundum ASD, of which six are familial ASD. The remaining 322 cases were sporadic, of which 24 individuals are diagnosed with ventricular septal defect among other CHDs (see Supplementary Material, Table S1 for details). Patients with syndromic CHDs and other developmental anomalies were excluded from the study.

Peripheral blood samples from all participants were collected after informed consent and the study is approved by the local ethical committees of Uppsala (project number 234/90) and Leicestershire (REC 6721). Consent was obtained from each individual or from the parents for individuals aged <18 years. DNA was extracted from blood using sodium dodecyl sulfate (SDS) and proteinase K treatment followed by phenol/chloroform extraction or using the QIAmp DNA blood Midi or Maxi kit from Qiagen. Human control DNA was obtained from the European Collection of Cell Culture (Sigma) and from anonymous Swedish blood donors.

Microsatellite marker genotyping

Fluorescent primers corresponding to the markers in Weber set version 6 (Cooperative Human Linkage Center) were used for amplification of polymorphic microsatellite repeats on all autosomes for the initial genome scan. For the fine-mapping of chromosome 15, the polymorphic microsatellite markers *D15S144* (UniSTS: 11942), *D15S1040* (UniSTS: 73677), *ACTC* (UniSTS: 64858), *D15S118* (UniSTS: 63940), *D15S659* (UniSTS: 58271) were used as well as the novel characterized microsatellites *GATA123322* and *GT44248*. The two latter repeats were identified in the sequenced bacterial artificial chromosome clone RP11–814P5 containing the *ACTC1* gene. The forward and reverse primer sequences used for the amplification of *GATA123322* and *GT44248* are (5′–3′) CCCTTATCTGAGCTGCTGTG, TTTTCTCCT GGGCATTCTTG and CAATTCCATCCTCCTCTGGA, CCCTTATCTGAGCTGCTGTG, respectively. We amplified the markers by polymerase chain reaction (PCR) as described previously (37). PCR products were pooled, diluted 100 times in de-ionized water and separated on a 3700 DNA Analyzer (Applied Biosystems, Foster City, CA, USA) and analyzed using GeneScan, version 3.1.3, and Genotyper, version 3.7 (Applied Biosystems), softwares. All microsatellite marker data and map distances were extracted using NCBI Map Viewer, Build 35 version 1 and Marshfield sex-averaged genetic map. The *ACTC1* gene sequence was derived from Genbank accession number NM_005159.1.

Haplotype and linkage analysis

Parametric two-point LOD score calculations were performed using the MLINK software, included in the FASTLINK package (version 5.1) assuming a dominant inheritance model and full penetrance. The disease incidence was set to 1/10 000. Haplotype construction of microsatellite marker alleles was performed manually and analyzed using the Cyrillic software, version 2.1.3 (Cherwell Scientific Publishing, Oxford, UK).

DNA sequencing

Exon amplicons for genomic sequencing of *ACTC1* were produced using 25 ng of genomic DNA, 1.5 mM $MgCl_2$, 0.2 μM of each primer, 50 μM dNTPs and 1 U Platinum® *Taq* DNA polymerase (Invitrogen, San Diego, CA, USA) with supplied buffer in 20 μl total volume. Amplified DNA was treated with 2 U Exonuclease I (Fermentas, Burlington, Canada) with supplied buffer and 0.5 U Calf intestine alkaline phosphatase (Fermentas) to digest excess dNTPs and un-incorporated DNA primers. Sequencing products were prepared using 5–20 ng PCR template, 1.6 pmol primer, 1 μl BigDye™ terminator version 3.1 reaction mixture (Applied Biosystems) with supplied buffer in a total volume of 10 μl and cycled at 94°C for 30 s; 25 cycles at (94°C, 25 s; 50°C, 15 s; 60°C for 2 min) followed by ethanol precipitation. In one patient with a secundum ASD showing a heterozygous 17 bp deletion, the sequence analysis was confirmed using cloned amplicons spanning exon 2 of *ACTC1*. PCR products were cloned into the pGEM-T vector system (Promega). Plasmids were isolated from transformed colonies by miniprep and positive clones containing the insert were sequenced as described above. DNA sequences of primers used for *ACTC1* re-sequencing are available upon request.

Denaturing high-performance liquid chromatography

Polymerase chain reactions were carried out using six pairs of primers designed with the assistance of primer 3 software to amplify the coding exons of *ACTC1*. (Primer sequences are available on request.) Following PCR amplification, the samples were put through a thermocycling program prior to analysis using the Transgenomic WAVE system for denaturing high-performance liquid chromatography (dHPLC). Optimal melting temperature for the *ACTC1* exon 2 PCR products was calculated using the dHPLC Melt Program (http://insertion.stanford.edu/melt.html). Five trays of control samples were analyzed using the same technique. To sequence the variants we carried out PCR on 60 ng of genomic DNA in a 50 μl reaction using standard protocols with Big Dye termin-

ator Sanger sequencing. Analysis was undertaken using Chromas Lite, version 2.01.

Expression and purification of recombinant actin

Site-directed mutagenesis was used to change the coding sequence of WT human *ACTC1* to M123V. The construct was fully sequenced to verify mutagenesis and the absence of PCR-induced errors. Expressed, purified protein was obtained using the baculovirus/Sf9 cell system according to previously reported protocols (8).

Actin-activated ATPase assay

The actin-activated ATPase activity of β-cardiac rabbit myosin (137 μg/ml) was determined at 30°C using various concentrations of the two recombinant actins (WT and M123V) in 10 mM imidazole, pH 7.0, 50 mM NaCl, 1 mM $MgCl_2$, 1 mM NaN_3 and 1 mM dithiothreitol (DTT). The assay was initiated by the addition of 2 mM MgATP and stopped with SDS at four time points every 10 min apart. The inorganic phosphate was determined colorimetrically as described previously (38).

Affinity of M123V cardiac actin for alpha-actinin

The relative binding of actin to alpha-actinin was determined with a competitive binding assay in a flow cell. The binding of TRITC (tetramethylrhodamine isothiocyanate)-phalloidin actin (M123V actin or tissue-purified skeletal actin) was competed with increasing amounts of unlabeled-phalloidin tissue-purified actin (22,39). A mixture of 5 μg/ml alpha-actinin and 0.5 mg/ml bovine serum albumin (BSA) was applied twice to each lane of a nitrocellulose-coated flow cell (38), and incubated for 1 min each time. The lanes were washed twice with buffer A [25 mM imidazole, pH 7.5, 50 mM KCl, 1 mM EGTA, 4 mM $MgCl_2$, 10 mM DTT, 1 mM MgATP, 2.9 mg/ml glucose, 0.125 mg/ml glucose oxidase (Sigma) and 0.023 mg/ml catalase (Sigma)]. Different ratios of fluorescent and unlabeled actin (constant 10 nM actin total) were applied twice for 1 min each, and then washed three times with buffer A. The percentage of bound, labeled filaments at each actin concentration was normalized to 100%-labeled actin run on a separate lane of the same flow cell. The density of the labeled actin was determined using ImageJ. An average of nine fields was analyzed per actin dilution.

In vitro motility assay

Actin filament velocity was measured at 30°C in motility buffer [25 mM imidazole, pH 7.5, 50 mM KCl, 1 mM EGTA, 4 mM $MgCl_2$, 10 mM DTT, 1 mM MgATP, 2.9 mg/ml glucose, 0.125 mg/ml glucose oxidase (Sigma), and 0.023 mg/ml catalase (Sigma) and 0.5% methylcellulose]. Cardiac myosin was prepared using an actin spin down to remove myosin that was unable to dissociate from actin in the presence of ATP, by mixing cardiac myosin (200 μg/ml) with an equimolar concentration of actin and 1 mM MgATP, followed by centrifugation (20 min at 350 000*g*). Cardiac myosin in the supernatant was applied to the nitrocellulose-coated flow cell (38) at 66 μg/ml, and the surface was blocked with 0.5 mg/ml BSA. Any remaining rigor heads were removed with an actin, ATP wash, in which 1 μM unlabeled, vortexed actin was added for 30 s, followed by a 1 mM MgATP wash. A weighted probability of the actin filament velocity for ~200 filaments was fitted to a Gaussian distribution and reported as a mean velocity ± SD for each experimental condition (40).

Application of fluorescently tagged MOs to chick embryos *in ovo*

To assess the effect of a reduction in expression of *ACTC1 in vivo*, we used a previously tested technique (6) to knockdown *ACTC1* in the developing chick heart. Initial experiments with analysis of transverse sections of chick hearts, which had been knocked down using *ACTC1* MO at a concentration of 500 μM, suggested an abnormality with bulboventricular looping. The experiment was subsequently repeated with analysis of the chick hearts in a sagittal section to more comprehensively show the looping pattern.

Antisense oligonucleotides (MOs) modified with fluorescent tags, designed to block initiation of transcription of *ACTC1*, were obtained from Gene Tools. The *ACTC1* MO was designed with a 3′-lissamine red-emitting tag. A second MO was designed with five mismatched bases distributed along the sequence to act as a control with a 3′-carboxyfluorescein green-emitting fluorescent tag. In addition, a standard control MO was used as a second control. MOs were made up to a final concentration of 15% F-127 pluronic gel (BASF Corp) in Hank's balanced salt solution to the appropriate concentration.

Fertile White Leghorn eggs (Henry Stewart) were incubated at 38°C for 50–51 h until HH Stage 13–14. A window was created in the shell, 5 ml of albumin was removed and the outer membrane removed from around the embryo. After staging a small hole was created next to the heart and 7 μl MO applied at a concentration of 400 μM at 4°C. At this temperature, the pluronic gel remains in the liquid state but solidifies at body temperature serving to keep the MO in place (41,42). Standard control MO (Gene Tools) was used at a concentration of 250 μM. The embryos were incubated *in ovo* for a further 31 h at 38°C before harvesting at Stage 20–21. After removal from the shell, extraneous membranes were removed, the fluorescence was checked using a Zeiss SV11 stereomicroscope and whole embryo photographs were taken.

We analyzed 13 embryos, in which fluorescence was present at Stage 20–21 indicating that the embryo had taken up the MO. Of these, seven were positive for the *ACTC1* MO and six were positive for the mismatch MO. We analyzed five WT embryos that were treated with pluronic gel/HBSS mix to assess only the normal range of development. We also analyzed three embryos treated with standard control MO as a second control group. Those embryos that had taken up the fluorescently labeled MO were fixed in 4% paraformaldehyde. The embryos were dehydrated in graded ethanol solutions and xylene before embedding in paraffin. Serial sections of 8-μm thickness were taken through the heart in a sagittal orientation. Sections were mounted on coated slides, de-waxed using xylene and put through graded

ethanol solutions to re-hydrate. At this stage we performed immunohistochemistry on some slides using a mouse monoclonal IgG antibody (Progen) recognized in chicken specific to *ACTC1*. Antigen retrieval was carried out by heating the slides in 10 mM sodium citrate in a microwave for 10 min at just below boiling point. Endogenous peroxidase activity was blocked using 1% hydrogen peroxide for 10 min before blocking with 5% normal goat serum for 1 h. The sections were incubated overnight in a 1:20 dilution of antibody at 4°C. After washing, the avidin–biotin phosphatase kit (Strep ABComplex/HRP duet Mouse/Rabbit kit, Dako) was used according to manufacturer's instructions to visualize the binding. The slides were then counterstained with Mayers Haemalum, dehydrated and mounted before analysis using a Zeiss Axioskop 2 microscope. The remaining slides were stained with Haemalum only without the immunohistochemistry steps.

ACKNOWLEDGEMENTS

The authors would like to thank the patients and families included in this report for their participation. We also thank Christin Hansson and Ulrika Gunnarsson for assistance with the genome scan.

Conflict of Interest statement. None declared.

FUNDING

This work has been financially supported by the Swedish Research Council (to N.D.), T. and R. Söderbergs Foundation, the Swedish Lung and Heart Foundation, Uppsala University and University Hospital, the British Heart Foundation and the National Institutes of Health.

REFERENCES

1. Hoffman, J.I. (1995) Incidence of congenital heart disease: I. Postnatal incidence. *Pediatr. Cardiol.* **16**, 103–113.
2. Benson, D.W., Sharkey, A., Fatkin, D., Lang, P., Basson, C.T., McDonough, B., Strauss, A.W., Seidman, J.G. and Seidman, C.E. (1998) Reduced penetrance, variable expressivity, and genetic heterogeneity of familial atrial septal defects. *Circulation*, **97**, 2043–2048.
3. Li, Q.Y., Newbury-Ecob, R.A., Terrett, J.A., Wilson, D.I., Curtis, A.R., Yi, C.H., Gebuhr, T., Bullen, P.J., Robson, S.C., Strachan, T. *et al.* (1997) Holt–Oram syndrome is caused by mutations in TBX5, a member of the Brachyury (T) gene family. *Nat. Genet.*, **15**, 21–29.
4. Schott, J.J., Benson, D.W., Basson, C.T., Pease, W., Silberbach, G.M., Moak, J.P., Maron, B.J., Seidman, C.E. and Seidman, J.G. (1998) Congenital heart disease caused by mutations in the transcription factor NKX2-5. *Science*, **281**, 108–111.
5. Garg, V., Kathiriya, I.S., Barnes, R., Schluterman, M.K., King, I.N., Butler, C.A., Rothrock, C.R., Eapen, R.S., Hirayama-Yamada, K., Joo, K. *et al.* (2003) GATA4 mutations cause human congenital heart defects and reveal an interaction with TBX5. *Nature*, **424**, 443–447.
6. Ching, Y.H., Ghosh, T.K., Cross, S.J., Packham, E.A., Honeyman, L., Loughna, S., Robinson, T.E., Dearlove, A.M., Ribas, G., Bonser, A.J. *et al.* (2005) Mutation in myosin heavy chain 6 causes atrial septal defect. *Nat. Genet.*, **37**, 423–428.
7. Rubenstein, P.A. (1990) The functional importance of multiple actin isoforms. *Bioessays*, **12**, 309–315.
8. Bookwalter, C.S. and Trybus, K.M. (2006) Functional consequences of a mutation in an expressed human alpha-cardiac actin at a site implicated in familial hypertrophic cardiomyopathy. *J. Biol. Chem.*, **281**, 16777–16784.
9. Hamburger, V. and Hamilton, H.L. (1992) A series of normal stages in the development of the chick embryo. 1951. *Dev. Dyn.*, **195**, 231–272.
10. Itasaki, N., Nakamura, H., Sumida, H. and Yasuda, M. (1991) Actin bundles on the right side in the caudal part of the heart tube play a role in dextro-looping in the embryonic chick heart. *Anat. Embryol. (Berl.)*, **183**, 29–39.
11. Latacha, K.S., Remond, M.C., Ramasubramanian, A., Chen, A.Y., Elson, E.L. and Taber, L.A. (2005) Role of actin polymerization in bending of the early heart tube. *Dev. Dyn.*, **233**, 1272–1286.
12. Erdogan, F., Ullmann, R., Chen, W., Schubert, M., Adolph, S., Hultschig, C., Kalscheuer, V., Ropers, H.H., Spaich, C. and Tzschach, A. (2007) Characterization of a 5.3 Mb deletion in 15q14 by comparative genomic hybridization using a whole genome 'tiling path' BAC array in a girl with heart defect, cleft palate, and developmental delay. *Am. J. Med. Genet. A*, **143**, 172–178.
13. Monserrat, L., Hermida-Prieto, M., Fernandez, X., Rodriguez, I., Dumont, C., Cazon, L., Cuesta, M.G., Gonzalez-Juanatey, C., Peteiro, J., Alvarez, N. *et al.* (2007) Mutation in the alpha-cardiac actin gene associated with apical hypertrophic cardiomyopathy, left ventricular non-compaction, and septal defects. *Eur. Heart J.*, **28**, 1953–1961.
14. Xu, C., Craig, R., Tobacman, L., Horowitz, R. and Lehman, W. (1999) Tropomyosin positions in regulated thin filaments revealed by cryoelectron microscopy. *Biophys. J.*, **77**, 985–992.
15. Olson, T.M., Michels, V.V., Thibodeau, S.N., Tai, Y.S. and Keating, M.T. (1998) Actin mutations in dilated cardiomyopathy, a heritable form of heart failure. *Science*, **280**, 750–752.
16. Mogensen, J., Klausen, I.C., Pedersen, A.K., Egeblad, H., Bross, P., Kruse, T.A., Gregersen, N., Hansen, P.S., Baandrup, U. and Borglum, A.D. (1999) Alpha-cardiac actin is a novel disease gene in familial hypertrophic cardiomyopathy. *J. Clin. Invest.*, **103**, R39–R43.
17. Olson, T.M., Doan, T.P., Kishimoto, N.Y., Whitby, F.G., Ackerman, M.J. and Fananapazir, L. (2000) Inherited and de novo mutations in the cardiac actin gene cause hypertrophic cardiomyopathy. *J. Mol. Cell. Cardiol.*, **32**, 1687–1694.
18. Van Driest, S.L., Ellsworth, E.G., Ommen, S.R., Tajik, A.J., Gersh, B.J. and Ackerman, M.J. (2003) Prevalence and spectrum of thin filament mutations in an outpatient referral population with hypertrophic cardiomyopathy. *Circulation*, **108**, 445–451.
19. Mogensen, J., Perrot, A., Andersen, P.S., Havndrup, O., Klausen, I.C., Christiansen, M., Bross, P., Egeblad, H., Bundgaard, H., Osterziel, K.J. *et al.* (2004) Clinical and genetic characteristics of alpha cardiac actin gene mutations in hypertrophic cardiomyopathy. *J. Med. Genet.*, **41**, e10.
20. Nowak, K.J., Wattanasirichaigoon, D., Goebel, H.H., Wilce, M., Pelin, K., Donner, K., Jacob, R.L., Hubner, C., Oexle, K., Anderson, J.R. *et al.* (1999) Mutations in the skeletal muscle alpha-actin gene in patients with actin myopathy and nemaline myopathy. *Nat. Genet.*, **23**, 208–212.
21. Kaindl, A.M., Ruschendorf, F., Krause, S., Goebel, H.H., Koehler, K., Becker, C., Pongratz, D., Muller-Hocker, J., Nurnberg, P., Stoltenburg-Didinger, G. *et al.* (2004) Missense mutations of ACTA1 cause dominant congenital myopathy with cores. *J. Med. Genet.*, **41**, 842–848.
22. D'Amico, A., Graziano, C., Pacileo, G., Petrini, S., Nowak, K.J., Boldrini, R., Jacques, A., Feng, J.J., Porfirio, B., Sewry, C.A. *et al.* (2006) Fatal hypertrophic cardiomyopathy and nemaline myopathy associated with ACTA1 K336E mutation. *Neuromuscul. Disord.*, **16**, 548–552.
23. Ilkovski, B., Cooper, S.T., Nowak, K., Ryan, M.M., Yang, N., Schnell, C., Durling, H.J., Roddick, L.G., Wilkinson, I., Kornberg, A.J. *et al.* (2001) Nemaline myopathy caused by mutations in the muscle alpha-skeletal-actin gene. *Am. J. Hum. Genet.*, **68**, 1333–1343.
24. Marston, S., Mirza, M., Abdulrazzak, H. and Sewry, C. (2004) Functional characterisation of a mutant actin (Met132Val) from a patient with nemaline myopathy. *Neuromuscul. Disord.*, **14**, 167–174.
25. Hogers, B., DeRuiter, M.C., Gittenberger-de Groot, A.C. and Poelmann, R.E. (1997) Unilateral vitelline vein ligation alters intracardiac blood flow patterns and morphogenesis in the chick embryo. *Circ. Res.*, **80**, 473–481.
26. Lamers, W.H. and Moorman, A.F. (2002) Cardiac septation: a late contribution of the embryonic primary myocardium to heart morphogenesis. *Circ. Res.*, **91**, 93–103.
27. Hove, J.R., Koster, R.W., Forouhar, A.S., Acevedo-Bolton, G., Fraser, S.E. and Gharib, M. (2003) Intracardiac fluid forces are an essential epigenetic factor for embryonic cardiogenesis. *Nature*, **421**, 172–177.
28. Kumar, A., Crawford, K., Close, L., Madison, M., Lorenz, J., Doetschman, T., Pawlowski, S., Duffy, J., Neumann, J., Robbins, J. *et al.*

(1997) Rescue of cardiac alpha-actin-deficient mice by enteric smooth muscle gamma-actin. *Proc. Natl. Acad. Sci. USA*, **94**, 4406–4411.
29. Abdelwahid, E., Pelliniemi, L.J., Szucsik, J.C., Lessard, J.L. and Jokinen, E. (2004) Cellular disorganization and extensive apoptosis in the developing heart of mice that lack cardiac muscle alpha-actin: apparent cause of perinatal death. *Pediatr. Res.*, **55**, 197–204.
30. Anderson, R.H., Brown, N.A. and Webb, S. (2002) Development and structure of the atrial septum. *Heart*, **88**, 104–110.
31. Boheler, K.R., Carrier, L., de la Bastie, D., Allen, P.D., Komajda, M., Mercadier, J.J. and Schwartz, K. (1991) Skeletal actin mRNA increases in the human heart during ontogenic development and is the major isoform of control and failing adult hearts. *J. Clin. Invest.*, **88**, 323–330.
32. Suurmeijer, A.J., Clement, S., Francesconi, A., Bocchi, L., Angelini, A., Van Veldhuisen, D.J., Spagnoli, L.G., Gabbiani, G. and Orlandi, A. (2003) Alpha-actin isoform distribution in normal and failing human heart: a morphological, morphometric, and biochemical study. *J. Pathol.*, **199**, 387–397.
33. Garner, I., Minty, A.J., Alonso, S., Barton, P.J. and Buckingham, M.E. (1986) A 5′ duplication of the alpha-cardiac actin gene in BALB/c mice is associated with abnormal levels of alpha-cardiac and alpha-skeletal actin mRNAs in adult cardiac tissue. *EMBO J.*, **5**, 2559–2567.
34. Nowak, K.J., Sewry, C.A., Navarro, C., Squier, W., Reina, C., Ricoy, J.R., Jayawant, S.S., Childs, A.M., Dobbie, J.A., Appleton, R.E. *et al.* (2006) Nemaline myopathy caused by absence of alpha-skeletal muscle actin. *Ann. Neurol*.
35. Gelernter-Yaniv, L. and Lorber, A. (2007) The familial form of atrial septal defect. *Acta Paediatr.*, **96**, 726–730.
36. Zetterqvist, P., Turesson, I., Johansson, B.W., Laurell, S. and Ohlsson, N.M. (1971) Dominant mode of inheritance in atrial septal defect. *Clin. Genet.*, **2**, 78–86.
37. Klar, J., Gedde-Dahl, T., Jr, Larsson, M., Pigg, M., Carlsson, B., Tentler, D., Vahlquist, A. and Dahl, N. (2004) Assignment of the locus for ichthyosis prematurity syndrome to chromosome 9q33.3–34.13. *J. Med. Genet.*, **41**, 208–212.
38. Trybus, K.M. (2000) Biochemical studies of myosin. *Methods*, **22**, 327–335.
39. Bing, W., Knott, A. and Marston, S.B. (2000) A simple method for measuring the relative force exerted by myosin on actin filaments in the in vitro motility assay: evidence that tropomyosin and troponin increase force in single thin filaments. *Biochem. J.*, **350** (Pt 3), 693–699.
40. Kinose, F., Wang, S.X., Kidambi, U.S., Moncman, C.L. and Winkelmann, D.A. (1996) Glycine 699 is pivotal for the motor activity of skeletal muscle myosin. *J. Cell. Biol.*, **134**, 895–909.
41. Becker, D.L., McGonnell, I., Makarenkova, H.P., Patel, K., Tickle, C., Lorimer, J. and Green, C.R. (1999) Roles for alpha 1 connexin in morphogenesis of chick embryos revealed using a novel antisense approach. *Dev. Genet.*, **24**, 33–42.
42. Becker, D.L. and Mobbs, P. (1999) Connexin alpha1 and cell proliferation in the developing chick retina. *Exp. Neurol.*, **156**, 326–332.